

Tunneling in NaBr:F⁻: Thermal and Dielectric Properties*

R. J. Rollefson[†]

Laboratory of Atomic and Solid State Physics, Cornell University, Ithaca, New York 14850

(Received 11 October 1971)

The existence of a large dipole moment and low-lying energy levels associated with the fluorine impurity ion in NaBr has been shown by measurements of paraelectric cooling, dielectric susceptibility, and low-temperature specific heat. Equilibrium orientations for the dipoles along the $\langle 110 \rangle$ directions have been deduced from measurements of the dielectric constant under applied stress and high-field polarization. Thermal-conductivity measurements indicate a rather long impurity-lattice relaxation rate. This has been confirmed by dielectric-relaxation measurements which give a relaxation rate which varies linearly with temperature below 5 K with a value of 10^5 sec^{-1} at 2 K. These observations are explained by means of a model in which the impurity ion tunnels between potential minima displaced from the lattice site, somewhat similar to the tunneling observed in KCl:Li⁺. Two major differences with the data for KCl:Li⁺, namely, a much broader specific-heat contribution and slower relaxation rate, necessitate a modification of the simple tunneling model used in describing KCl:Li⁺. By taking into account the effect of lattice strains on the tunneling motion, good agreement is obtained with the data for NaBr:F⁻. Using this model a value of 8.7 mK is calculated for the tunneling matrix element. Thus NaBr:F⁻ represents a tunneling system in the limit of a small tunneling matrix element while KCl:Li⁺ is characteristic of a large tunneling matrix element. Evidence is cited for other systems which might fit the strained tunneling model. These systems are RbCl:Ag⁺, RbCl:OH⁻, and KCl:OH⁻.

I. INTRODUCTION

Impurities in ionic crystals which can reorient at low temperatures by tunneling have been the object of considerable experimental and theoretical investigation during the past ten years.¹ Quantum-mechanical tunneling produces a splitting of the orientational degeneracy analogous to the inversion splitting of the ammonia molecule. The resulting closely spaced energy levels give rise to a number of unusual low-temperature properties. A particularly novel mode is exhibited by the monatomic impurity ion Li⁺ in KCl. It has been shown that the lithium ion tunnels between potential minima displaced from the center of the lattice cavity in the $\langle 111 \rangle$ directions. A large dipole moment associated with the displaced lithium ion makes possible the manipulation of the ion's orientation by means of electric fields.

The interest in the present work is twofold. First of all, since KCl:Li⁺ represents the only off-center impurity which has been studied extensively, it is of interest to investigate another system exhibiting the same type of behavior to establish the tunneling model as one which may occur with some generality in solids. Secondly, if a system with a small tunnel splitting and large dipole moment could be found, it might have the potential of conveniently producing very low temperatures by means of paraelectric cooling. A small tunnel splitting might also make possible observation of effects masked by the large tunnel splitting of KCl:Li⁺.

A search was made for off-center impurity ions

in a number of alkali halide systems using paraelectric cooling as a test. Similar efforts have also been undertaken by Kapphan and co-workers² and Lombardo and Pohl.³ Most of the systems tested gave negative results. These are nevertheless of interest since the occurrence of paraelectric cooling is one of the most straightforward tests for mobile off-center ions, and the possible existence of off-center ions in a number of these systems has been in question. A listing of the results thus far obtained is given in Table I.

TABLE I. Alkali halide systems tested for paraelectric cooling.

Positive results		
KCl:Li ⁺ ^a	RbCl:Ag ⁺ ^b	NaBr:F ⁻ ^{c,d}
Negative results		
NaCl:Li ⁺ ^e	KCl:Rb ⁺ ^a	RbCl:Li ⁺ ^{e,f}
:Cu ⁺ ^e	:Ag ⁺ ^a	:Na ⁺ ^f
:F ⁻ ^c	:Cu ⁺ ^{c,e}	:K ⁺ ^c
NaBr:Li ⁺ ^c	:F ⁻ ^d	:Cu ⁺ ^c
	:e ⁻ ^a	:F ⁻ ^c
	KBr:Li ⁺ ^{d,e}	RbBr:Ag ⁺ ^b
	:Cu ⁺ ^c	RbI:Ag ⁺ ^c
	:H ⁻ ^a	CsBr:Na ⁺ ^e

^aReference 17.

^bReference 41.

^cPresent work.

^dReference 3.

^eReference 2.

^fG. Lombardo, Ph. D. thesis (Cornell University, 1971) (unpublished).

The system chosen for more extensive study was NaBr doped with NaF. Preliminary observations by Lombardo and Pohl³ of paraelectric cooling indicated that the fluorine ions may occupy off-center positions. A systematic study of NaBr : F⁻ was undertaken employing measurements of specific heat, paraelectric cooling, thermal conductivity, and dielectric relaxation, the results of which are reported here. In Sec. II the experimental results are presented preceded by a brief description of apparatus and technique. Section III begins with considerations leading to a modification of the simple tunneling model used for KCl : Li⁺, followed by a comparison of the model with the experimental results for NaBr : F⁻. In Sec. IV data for RbCl : Ag⁺, RbCl : OH⁻, and KCl : OH⁻ are discussed and similarities between these data and the modified tunneling model are noted. Section V contains a summary and conclusions.

II. EXPERIMENT

A. Experimental Details

The measurements described below were performed in several different cryostats. Between 0.05 and 2 K an adiabatic-demagnetization cryostat⁴ was used for all measurements except paraelectric cooling and dielectric relaxation which were performed in a He³ cryostat⁵ operating to 0.28 K. At higher temperatures a He⁴ conduction cryostat,⁶ modified by the addition of a bellows-type heat switch,⁷ was used for measurements of specific heat, thermal conductivity, and paraelectric cooling, while the high-field polarization and dielectric constant under stress were measured in He⁴ immersion cryostats.

Standard procedures outlined in previous publications^{4-6,8} were used in measuring the specific heat, thermal conductivity, and paraelectric cooling. The permanent thermal link between the sample and post required for the low-temperature specific-heat measurements was provided by a thin copper wire attached to a metallic area contact on the sample. The large heat capacity at low temperatures necessitated a large area to avoid contact resistance. Gold films evaporated to a thickness several times opacity provided the most reliable contacts, with the wire attached to the film using Dupont electric-grade-4922 silver paint.

The dc dielectric constant was measured on a circuit described by Fiory.⁹ Briefly, a constant voltage supplied by a 5.4-V mercury battery was applied to the series connection of a large fixed capacitor and the sample capacitance. The voltage across the fixed capacitor was then measured with an electrometer. This voltage was related to the dielectric constant using the capacitance of the fixed capacitor, the applied voltage, and the sample

thickness and electrode area.

The same circuit was used to measure the high-field polarization. In this case the voltage was supplied by a Hewlett-Packard precision high-voltage supply operating at voltages of up to 3000 V. To increase the accuracy of the readings the output of the electrometer was fed into a Heath digital voltmeter. As a check on the measuring equipment, and to facilitate subtraction of the pure-crystal contribution to the polarization, an undoped NaBr crystal was measured. The polarization was found to be linear to within $\pm 0.25\%$.

A General Radio capacitance bridge was used for the ac dielectric-constant measurements, operated in the three-terminal configuration. The bridge was designed to operate at frequencies less than 100 kHz, which was the upper limit of the narrow-band amplifier and null detector used for zeroing. By amplifying the signal from the bridge with a Tectronics wide-band amplifier and displaying it on an oscilloscope, it was possible to determine a reasonably good null for the bridge up to frequencies of 600 kHz. At these frequencies stray capacitance and inductance in the bridge introduced considerable errors, but useful qualitative results were still obtainable. In all dielectric measurements carefully shielded cables minimized stray capacitance effects in the leads.

For measurements with applied stress a thin slab sample was pressed between blocks of pure NaBr, as shown in Fig. 1. The faces of the blocks and sample in contact were of the same crystallographic orientation to eliminate spurious strains. Gold electrodes were evaporated onto the faces of the

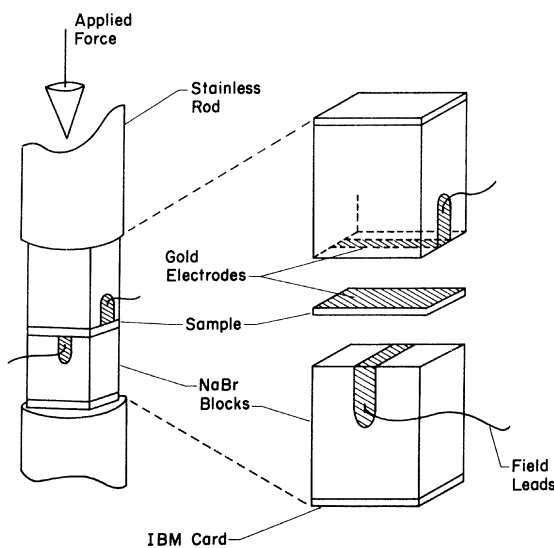


FIG. 1. Mounting of sample for measurement of dielectric constant in applied stress.

crystal with electrical contact made by gold strips evaporated across the faces of the blocks. A check for hysteresis in the stressing apparatus was made by repeating points for increasing and decreasing stress. Good reproducibility was observed.

Primary thermometry in all cryostats was provided by germanium resistance thermometers originally calibrated against a platinum thermometer, He⁴ and He³ vapor pressures, and a cerium-magnesium-nitrate salt pill. Carbon resistors provided convenient secondary thermometry. Resistance thermometers were measured with an ac bridge described by Seward.⁵

The crystals were seed pulled from bromine-treated pyrolytic-graphite crucibles in vacuum-tight stainless-steel furnaces under a high-purity-argon protective atmosphere.¹⁰ Bromine-treated Merck Ultra Pure powder from the Merck Chemical Co. (Darmstadt, Germany) was used as the starting material. Considerable care had to be exercised in handling the crystals due to the hygroscopic nature of NaBr. By maintaining the relative humidity of the room below 40% and surrounding the work area with heat lamps, a cleaved surface could be kept clean and shiny indefinitely. To relieve strains caused by cleaving and grinding the crystals were annealed in a silica boat in vacuum at 500 °C for 15–30 min and then cooled slowly.

Analysis for fluorine-ion content was carried out by the Materials Science Center Analytic Facility using the specific-ion-electrode method. This method of analysis is very sensitive to fluorine-ion concentration, giving an accuracy of a few percent. However, fluctuations in concentration occur within a crystal boule, and thus an uncertainty in the fluorine concentration of a particular sample still exists as not all samples cut from a single boule are analyzed individually. In order to minimize the variation in fluorine-ion concentration the samples used for the high-field polarization were all cut from the same region of a large boule.

Unwanted OH⁻ impurities present a considerable difficulty in alkali halide crystals, particularly NaBr. Although great care was exercised in growing the present crystals, there was some OH⁻ contamination. An approximate determination of OH⁻ ion concentration was made using uv absorption at 77 K.¹¹ As a check for any other impurities, two samples were given an impurity survey using emission spectrography. The impurity concentrations for all crystals used are given in Table II.

As a check to ensure that the fluorine ions were entering the lattice substitutionally and not interstitially the ionic conductivities of a pure sample and a fluorine-ion-doped sample ($1.8 \times 10^{18} \text{ cm}^{-3}$) were measured in an apparatus described by O'Brien.¹² No increase in the conductivity of the doped sample over that of the pure was observed,

indicating a substitutional placement.

The interest in the heat-capacity measurements was due to the contribution of the fluorine ions. Therefore, the specific heat of a pure NaBr sample was measured so that this could be subtracted from the total specific heat of the fluorine-doped samples. Below about 1 K the specific heat of a pure alkali halide obeys the Debye equation, with a T^3 temperature dependence. The Debye temperature was calculated from the specific-heat measurements using the equation¹³

$$C_v/Nk = 234(T/\Theta_D)^3 \quad ,$$

with the results shown in Fig. 2. A low-temperature limit of 215 K was found for Θ_D . The slight decrease of Θ_D at the lowest temperatures is likely caused by residual impurities. Tunneling impurities in concentrations of less than 0.1 ppm would be sufficient to cause the observed deviation. The value of 215 K for Θ_D is substantially less than that of ultrasonic experiments,¹⁴ where Θ_D is calculated to be 224.6 K. It is unlikely that residual impurities could account for this discrepancy, since their effect would be negligible by 1 K. It might be noted that similar discrepancies have been observed before, for example in NaF,¹⁵ with no adequate explanation having yet been found.

B. Data

In considering the data obtained for NaBr : F⁻ it is useful to have in mind the properties of the simple tunneling model used so successfully in describing

TABLE II. Crystal boules, $N_{\text{NaBr}} = 1.88 \times 10^{22}$ molecules/cm³. The concentration of fluorine grown into the crystal (column 3) is only a small fraction of the concentration in the melt (column 2).

Boule number	mole %		
	NaF in melt	$N_{\text{F}}(\text{cm}^{-3})$	$N_{\text{OH}}(\text{cm}^{-3})$
809161W			0.2×10^{16}
812121W	0.01	9.0×10^{16}	0.4×10^{16}
811011W	0.1	7.7×10^{17}	0.9×10^{16}
810281W	0.2	1.3×10^{18}	0.9×10^{16}
809261W	0.5	1.8×10^{18}	1.3×10^{16}
901281W	1.0	5.1×10^{18}	1.5×10^{16}
441	1.0	5.5×10^{18}	6×10^{16}

Spectroscopic analysis		
Element detected	Estimated concentration (ppm)	
	Boule No. 809161W	Boule No. 809261W
Mg	1–10	1–10
Al	1–10	1–10
Cu	1–10	1–10
K	10–100	10–100
Ca	1–10	1–10
Ag	...	0.1–1
Ti	...	0.1–1

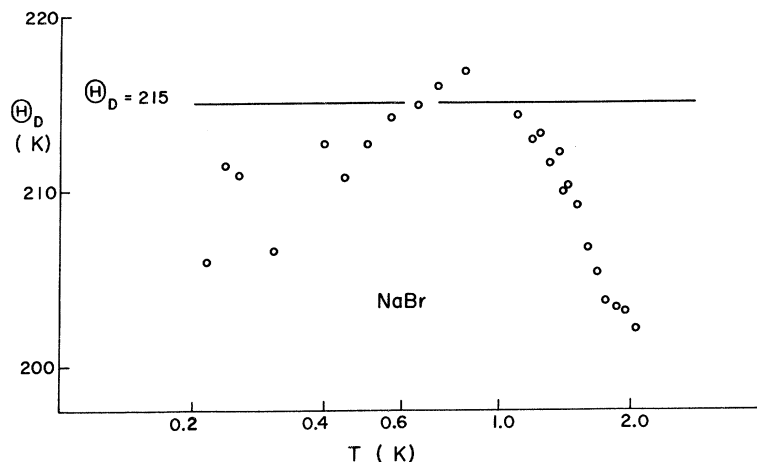


FIG. 2. Temperature dependence of Θ_D for NaBr.

the KCl:Li⁺ system.¹⁶ Although the model used for KCl:Li⁺ involves tunneling between eight equivalent wells, the qualitative features of interest here can be seen in the simple double-well harmonic-oscillator model. This model is discussed more thoroughly in Sec. III, and its properties will merely be summarized here. Quantum-mechanical tunneling through the barrier between the wells splits the doubly degenerate ground state of the system into two levels, with a splitting given by twice the tunneling matrix element. The eigenstates are the symmetric and antisymmetric combinations of the single-well wave functions and give rise to a Schottky specific-heat anomaly. The application of an electric field will tend to localize the ion in one well, inducing a dipole moment. By taking a thermal average of the states the average induced moment can be calculated. For temperatures large compared with the ground-state splitting the susceptibility obeys the Langevin-Debye equation. At lower temperatures saturation occurs at a value of the susceptibility equal to the polarizability of the lowest energy state. The temperature-dependent susceptibility makes possible the observation of paraelectric cooling by adiabatic removal of an electric field.

In the KCl:Li⁺ system early measurements of paraelectric cooling¹⁷ and dielectric constant¹⁸ indicated that the lithium ions made a Langevin-Debye contribution to the susceptibility which led to the proposal that the lithium occupies an off-center position. Preliminary observations³ of paraelectric cooling in NaBr:F⁻ at 4.6 K indicated that here, too, the impurity ion may be off-center.

In Fig. 3 the paraelectric cooling¹⁹ is shown as a function of temperature for two values of electric field and fluorine-ion concentration. The shapes of these curves are qualitatively similar to those observed for KCl:Li⁺.⁸ At the highest temperatures the cooling approaches a T^{-4} dependence indicated

by the solid lines. Such a dependence indicates a susceptibility varying as T^{-1} , where the cooling is given by⁸

$$\Delta T = N_F \mu_0^2 E^2 / 6 A k T^4,$$

where E is the applied electric field, N_F the chemically determined number of dipoles in the field, μ_0 the dipole moment, and $A T^3$ the lattice specific heat. From this expression a value for the dipole moment can be calculated with the results $\mu_0 = 3.4$ D for the low-concentration sample and $\mu_0 = 3.9$ D for the high-concentration sample, uncorrected for local field (1 D = 10^{-18} esu). These values represent a lower limit since true T^{-4} behavior has not yet been reached at these temperatures. (See the discussion of dipole moment in connection with the dielectric-constant and high-field-polarization mea-

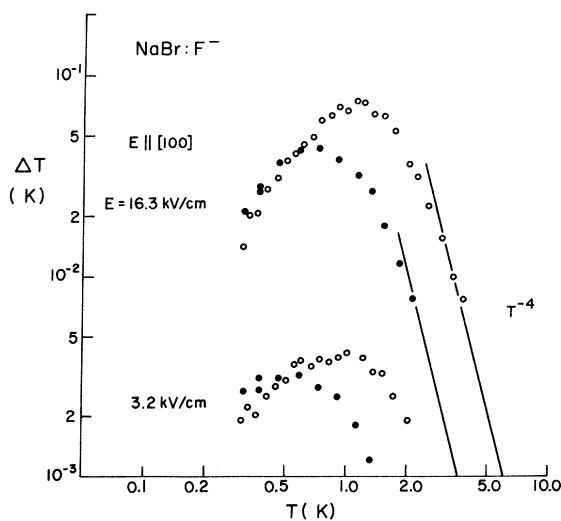


FIG. 3. Paraelectric cooling of NaBr:F⁻. Open circles: $N_F = 5.1 \times 10^{18} \text{ cm}^{-3}$; closed circles: $N_F = 7.7 \times 10^{17} \text{ cm}^{-3}$.

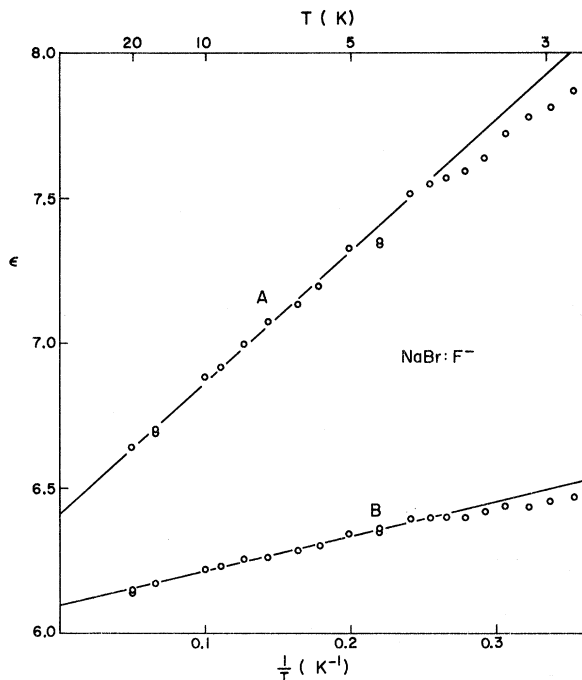


FIG. 4. dc dielectric constant of NaBr : F⁻. (A) $N_F = 5.5 \times 10^{18} \text{ cm}^{-3}$; (B) $N_F = 1.8 \times 10^{18} \text{ cm}^{-3}$.

measurements below.)

At the higher temperatures the cooling varies approximately linearly with concentration indicating that the fluorine ions are acting independently. At low temperatures the cooling becomes independent of concentration. This results from the fact that the low-lying energy levels of the fluorine ions are dominating the specific heat and the ions are merely cooling themselves. A more complete discussion of the temperature dependence of paraelectric cooling in tunneling systems may be found in the paper by Pohl *et al.*⁸ At present we merely note that the dependence observed for NaBr : F⁻ is that expected for a tunneling impurity.

To get a more direct measure of the polarizability the dc dielectric constant of NaBr : F⁻ was measured as a function of temperature from 80 mK to 20 K. Thin-slab crystals with two different fluorine-ion concentrations were used. A plot of the measured dielectric constant as a function of T^{-1} gives a straight line with positive slope for small values of T^{-1} (Fig. 4). At temperatures below 20 K the host dielectric constant is temperature independent and thus the data indicate that the fluorine ions are making a contribution varying inversely with temperature. From the extrapolated vertical axis intercept the host dielectric constant can be determined, with values of 6.1 and 6.4 for the low- and high-concentration samples, respectively. This discrepancy is within the limits of uncertainty in

the electrode area. For a Langevin-Debye polarizability the slope of the line is given by $N_F \mu_0^2 / 3k$. Using the chemically determined value of N_F , the dipole moment is calculated to be 4.7 D for the low-concentration sample and 5.1 D for the high-concentration sample. An uncertainty of 10% in these values arises from uncertainties in the electrode area and the fluorine-ion concentration. The values of μ_0 calculated here are larger than those calculated from the paraelectric-cooling data. As noted above this may be due to the fact that the cooling was not observed in the temperature range of true Langevin-Debye polarizability. The question of the correct value for the dipole moment will arise again in the discussion of the high-field-polarization data.

By subtracting the contribution of the pure crystal from the total dielectric constant the change caused by the fluorine ions is obtained (see Fig. 5). Below about 4 K this contribution begins to level off indicating that the thermal energy is comparable to the fluorine-ion ground-state splitting. For the higher concentration the dielectric constant is actually seen to pass through a maximum, decreasing slightly at lower temperatures. This behavior has been observed for a number of electric-dipole systems and is attributed to electric dipole-dipole interactions, as discussed in a recent paper by Fiory.⁹ The effect is still very small for the highest concentration used in the present experiments.

This dielectric behavior lends strong support to the original contention, based on paraelectric cooling, that the fluorine ion tunnels between off-center potential minima. A measurement of the specific heat should therefore yield a Schottky contribution from which a value for the tunneling matrix element could be calculated. The specific heat was measured¹⁹ for several fluorine-ion concentrations varying between 9×10^{16} and $5.5 \times 10^{18} \text{ cm}^{-3}$ (see Fig. 6). A large contribution to the low-temperature specific heat is indeed observed, which increases with the fluorine-ion content. However, the shape of the excess contribution is clearly not that of a Schottky anomaly. At the lowest temperatures the present data decrease linearly in T rather than exponentially as observed in KCl : Li⁺.²⁰ At these low temperatures the pure-lattice contribution to the specific heat is negligible. This is the first clear evidence of a difference between these two systems.

The excess specific heat, obtained by subtraction of the pure-crystal specific heat (Fig. 7), exhibits a peak at temperatures slightly less than 1 K, indicating the presence of energy levels with a splitting on the order of 1 K in temperature units. The dashed line in the figure shows the temperature dependence of a Schottky term, which by 0.1 K has fallen several orders of magnitude below the present data. From this it is clear that the evaluation of the specific-heat data in terms of a tunneling

matrix element, as was done for $\text{KCl}:\text{Li}^+$, is not justified in the present case. This is also indicated by the fact that the temperature at which the peak occurs increases as the fluorine-ion concentration increases. If the peak temperature were determined by the tunneling matrix element, it would be the same for all concentrations, as observed in $\text{KCl}:\text{Li}^+$.

The entropy associated with the specific-heat peak was calculated by computing the area under a plot of $(C_{\text{total}} - C_{\text{pure}})T^{-1}$ vs T . As shown in Fig. 8 the entropy divided by $N_F k$ is nearly independent of fluorine-ion concentration, increasing from 1.05 to 1.66 as the concentration increases by a factor of 60.

Another probe of the low-lying energy levels which had proved useful in $\text{KCl}:\text{Li}^+$ was the thermal conductivity.²¹ The lithium impurity ions are strong resonant scatterers of phonons, with ion concentrations of 10^{18} cm^{-3} causing a decrease in the thermal conductivity at 1 K of nearly two orders of magnitude. However, in NaBr no effect of doping with NaF was observable in the thermal conductivity. The data for pure NaBr and two rather heavily doped $\text{NaBr}:\text{F}^-$ samples are shown in Fig. 9. Both the pure sample and the fluorine-doped samples show a slight decrease below the T^3 behavior observed for very pure alkali halides at low temperatures. The decrease scales approximately with OH^- concentration and is therefore probably due to this impurity which is a known phonon scatterer.²² It should be pointed out that these OH^- concentrations are two

orders of magnitude too small to account for the large specific heat and dielectric contributions described above.

It is concluded, therefore, that although there are states of comparable energy splitting in both $\text{KCl}:\text{Li}^+$ and $\text{NaBr}:\text{F}^-$, as evidenced by the specific heat, in $\text{NaBr}:\text{F}^-$ the phonon scattering of these states is smaller by at least three orders of magnitude. Since the phonon-scattering strength is proportional to the impurity-lattice relaxation rate the lack of observable phonon scattering for $\text{NaBr}:\text{F}^-$ implies a relaxation rate three orders of magnitude slower than that of the lithium ion in KCl . This is the second major experimental difference between the two systems.

By means of low-temperature dielectric-relaxation measurements it was possible to directly determine the relaxation rate in $\text{NaBr}:\text{F}^-$,²³ something which has proven difficult in $\text{KCl}:\text{Li}^+$ due to its very fast relaxation.²⁴ This same method, i.e., dielectric relaxation, has been used for the tunneling system $\text{KCl}:\text{OH}^-$,²⁵ but the high frequencies required for this system made the measurements rather difficult. In Fig. 10 the real part of the dielectric constant at four frequencies is plotted as a function of temperature. The host dielectric constant is frequency independent in this range, and thus the change in ϵ' as a function of frequency reflects the change in the fluorine-ion contribution to the dielectric constant. At a frequency of 100 kHz this contribution has been reduced nearly to zero, indicating that at these frequencies the fluorine ion is unable

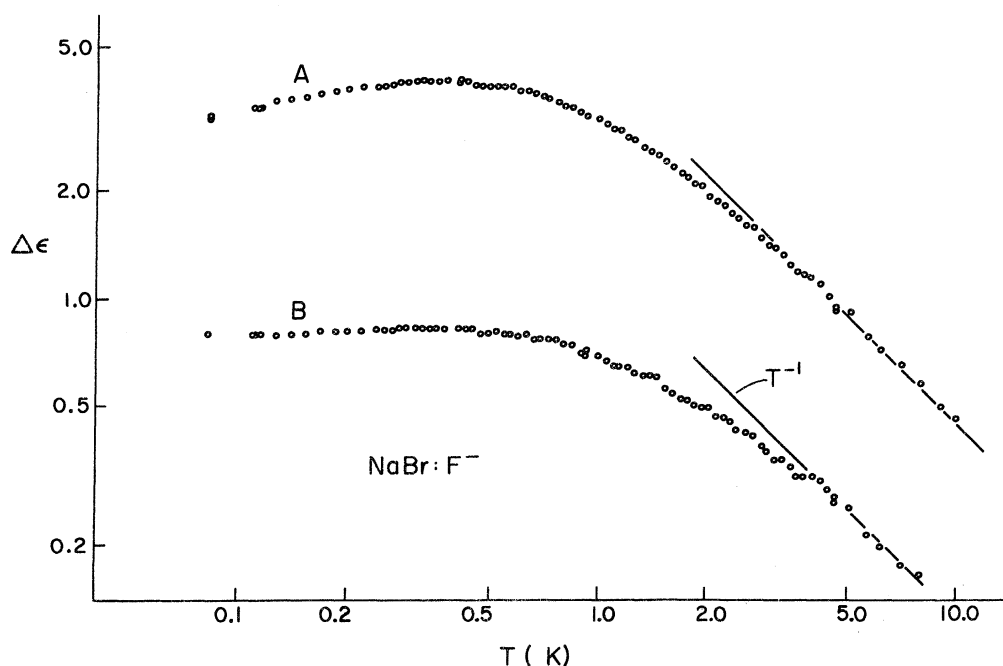


FIG. 5. Fluorine-ion contribution to the dc dielectric constant of $\text{NaBr}:\text{F}^-$. Concentrations as in Fig. 4.

to follow the rapidly changing electric field. Thus a relaxation rate on the order of 10^5 sec^{-1} is indicated.

The frequency dependence is seen more clearly by plotting the real and imaginary parts of the dielectric constant as a function of frequency, as

shown in Fig. 11 for $T = 2.1 \text{ K}$. The relaxation appears to be of the Debye type, with the real part of the dielectric constant decreasing smoothly while the imaginary part passes through a maximum. A more accurate check on the Debye character of the relaxation is provided by a plot of ϵ'' vs ϵ' , often

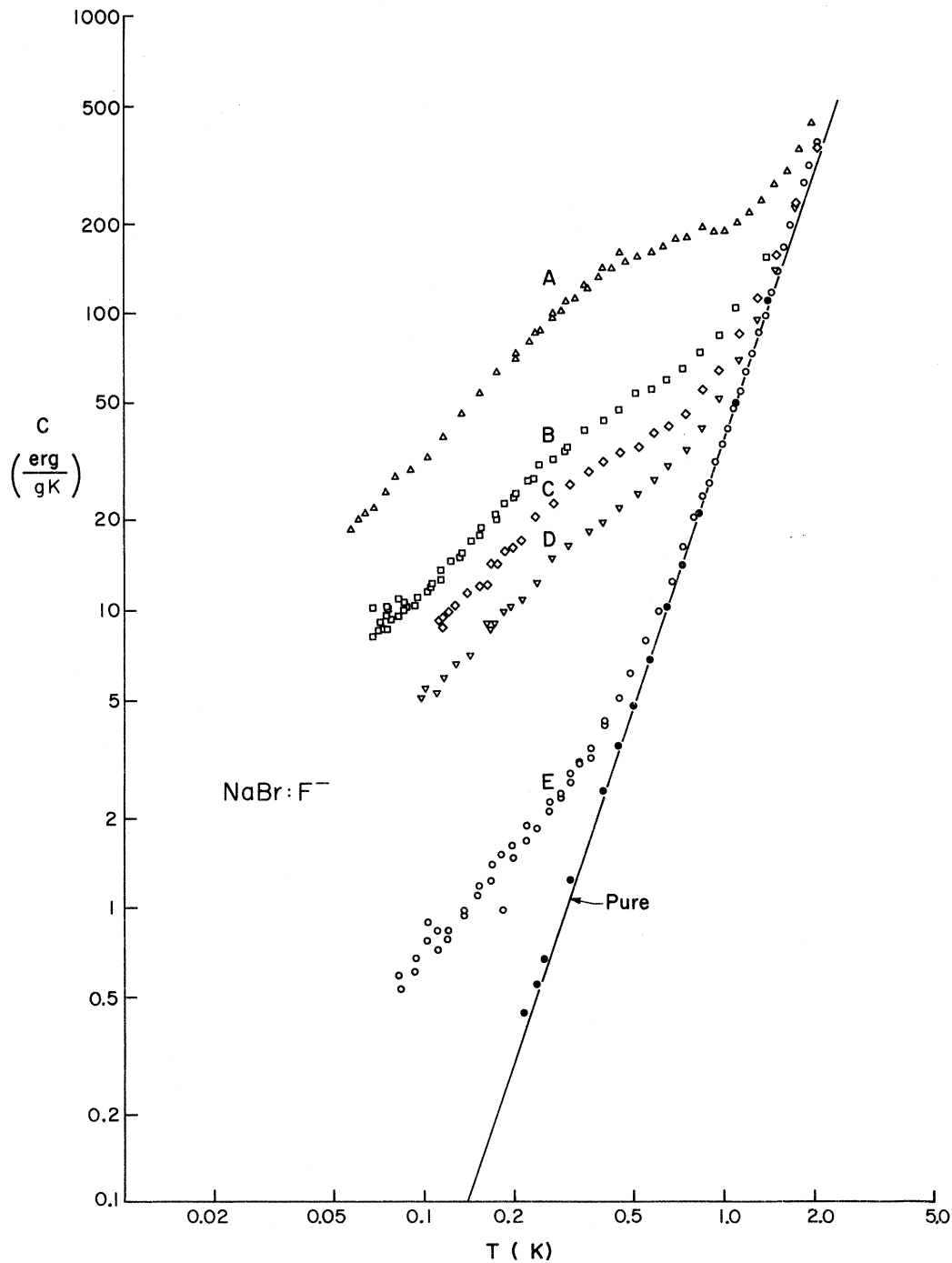


FIG. 6. Specific heat of NaBr:F⁻. (A) $N_F = 5.5 \times 10^{18} \text{ cm}^{-3}$; (B) $N_F = 1.8 \times 10^{18} \text{ cm}^{-3}$; (C) $N_F = 1.3 \times 10^{18} \text{ cm}^{-3}$; (D) $N_F = 7.7 \times 10^{17} \text{ cm}^{-3}$; (E) $N_F = 9.0 \times 10^{16} \text{ cm}^{-3}$.

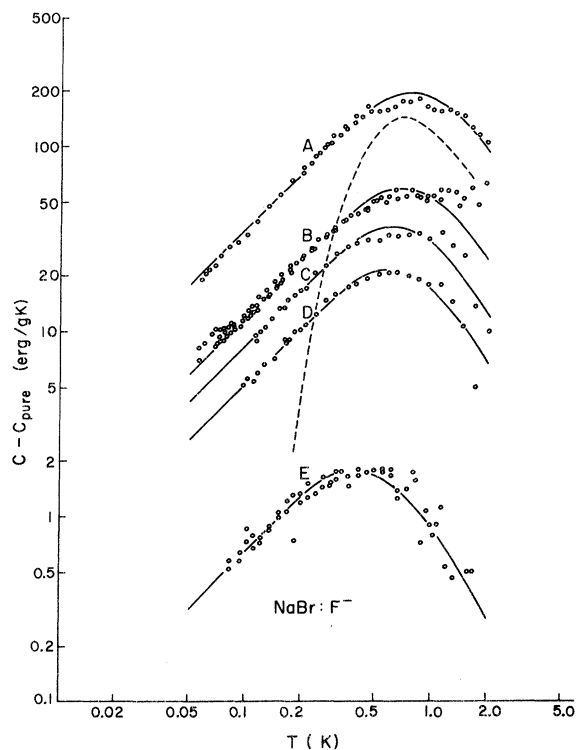


FIG. 7. Specific heat of NaBr:F⁻ with pure-crystal contribution subtracted. Concentrations the same as Fig. 6. Dotted line shows temperature dependence of Schottky term. Solid lines were calculated using a distribution of energy level splittings as discussed in Sec. III.

called a Cole-Cole plot²⁶ (see Fig. 12). The circular character of the plot with the center of the circle somewhat below the horizontal axis is characteristic of a Debye relaxation with a small spread of relaxation rates.

The average relaxation rate at each temperature was determined by noting the value of ϵ' corresponding

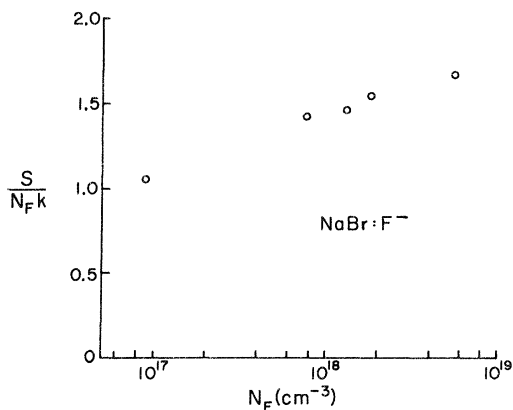


FIG. 8. Fluorine-ion contribution to the entropy of NaBr:F⁻ as a function of concentration.

to the center of the circle in plots such as Fig. 12 and determining the frequency at which this value of ϵ' was observed. The resulting temperature dependence of the relaxation rate is shown in Fig. 13. Below 5 K the relaxation rate (in sec⁻¹) is approximately proportional to T (in K), i.e.,

$$1/\tau = 5.8 \times 10^4 T.$$

Similar measurements were made for a sample with $N_F = 7.7 \times 10^{17}$ cm⁻³ with results in agreement with the above to within 20%. In contrast to this, the relaxation rate for KCl:Li⁺ at 1 K is at least 10^8 sec⁻¹.²⁴ The difference of more than three orders of magnitude explains the lack of observable phonon scattering in NaBr:F⁻.

The dielectric measurements discussed so far indicate that a rotating dipole moment is associated with the fluorine ion. Since the dipole rotates in a cubic lattice, it would be expected to have equilibrium orientations determined by the cubic crystal field. Only three sets of orientations are likely: the six $\langle 100 \rangle$ directions, the eight $\langle 111 \rangle$ directions, or the twelve $\langle 110 \rangle$ directions. Two experiments were undertaken to distinguish between these three

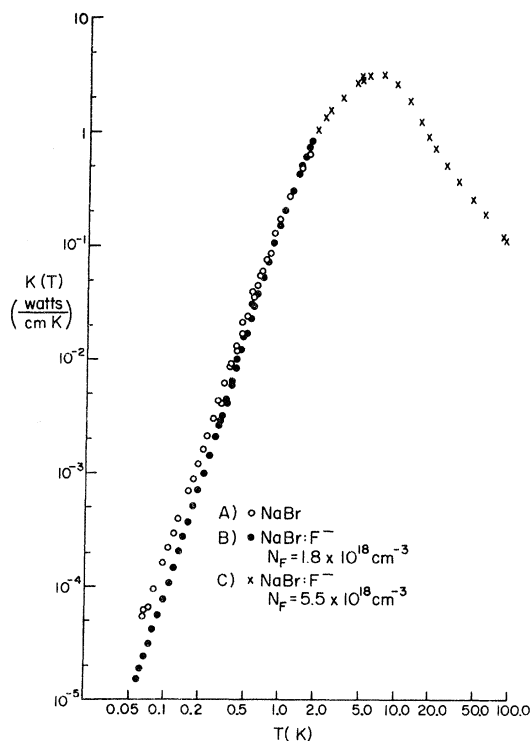


FIG. 9. Thermal conductivity of NaBr and NaBr:F⁻. The data for sample C below 1.5 K are identical with those for sample B and are omitted for clarity. The difference between the conductivities of the pure and doped samples at the lowest temperatures is probably due to different residual OH⁻ contamination. See text.

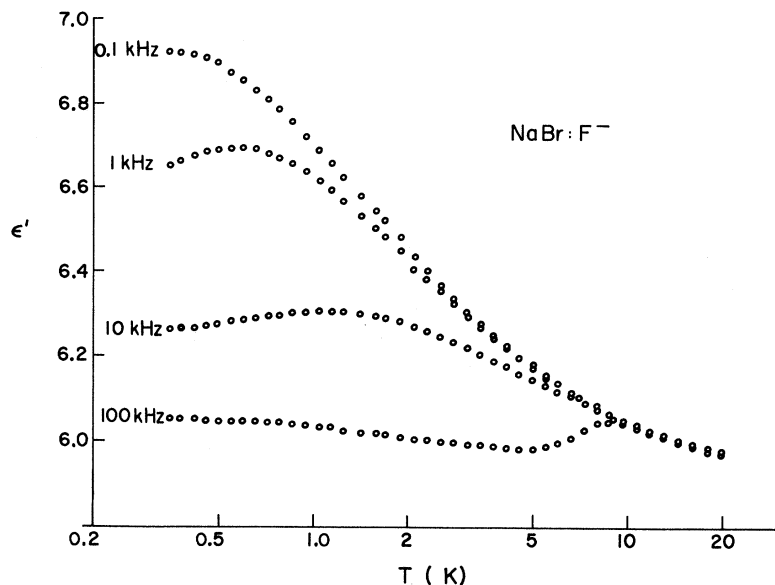


FIG. 10. ϵ' of NaBr : F⁻ vs temperature. $N_F = 1.8 \times 10^{18} \text{ cm}^{-3}$.

possibilities.

In the first experiment the polarization was measured as a function of crystallographic orientation in fields up to 100 kV/cm. At high fields the polarization will saturate at a value determined by the component of the fluorine dipole moment along the field, which will depend on the equilibrium dipole orientations.

The polarization of the doped samples after subtraction of the pure-crystal contribution is shown in Fig. 14 for electric fields in the [110], [111], and [100] directions. The short horizontal lines at the right of the figure indicate the relative spacings for

saturation polarization if the dipole is constrained to the $\langle 110 \rangle$ orientations. The data are seen to be consistent with $\langle 110 \rangle$ orientations although the spacings are not quite right. This may in part be due to a lack of full saturation of the polarization.

If it is assumed that the [110] polarization is saturated at a value of $N_F \mu_0$, the dipole moment calculated using the chemically determined value of N_F is 3.5 D. This is comparable to the values calculated from the paraelectric-cooling data and substantially less than the values calculated from the dielectric-constant measurements. It seems unlikely that a lack of saturation could be sufficient

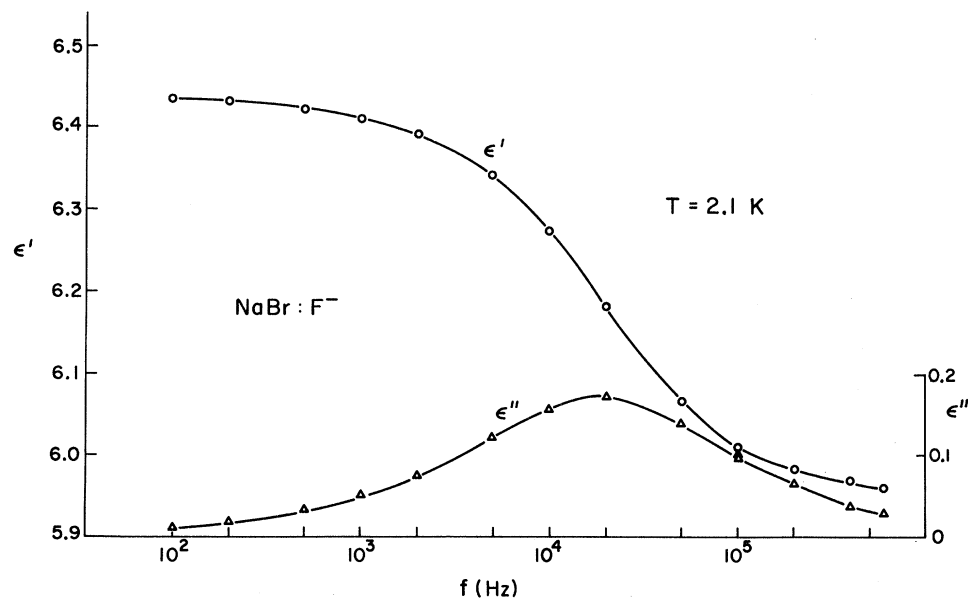


FIG. 11. ϵ' and ϵ'' for NaBr : F⁻ as a function of frequency. $N_F = 1.8 \times 10^{18} \text{ cm}^{-3}$.

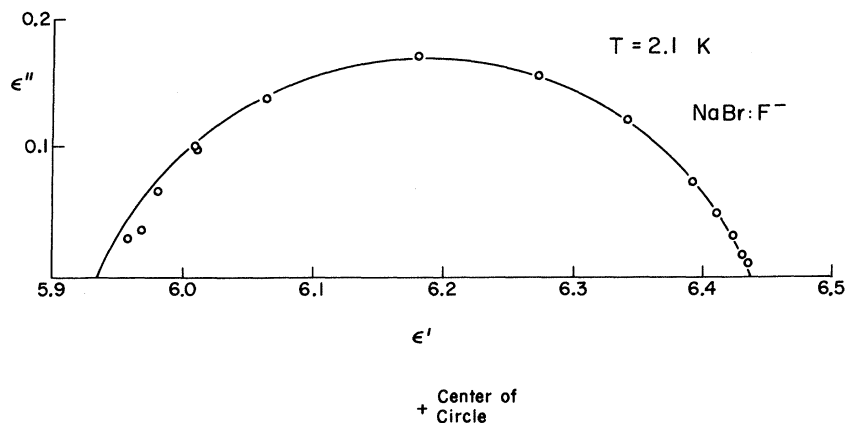


FIG. 12. Cole-Cole plot for dielectric relaxation in NaBr:F⁻. $N_F = 1.8 \times 10^{18} \text{ cm}^{-3}$.

to explain the discrepancy with the dielectric-constant data and equally unlikely that the fluorine-ion concentration could be so much in error. It would seem, therefore, that two values of the dipole moment are measured, one for fields greater than 3 or 4 kV/cm as in the paraelectric-cooling and high-field-polarization experiments, and one for fields on the order of 0.1 kV/cm as in the dielectric-constant measurement. The significance of this observation is not clear at present.

The second method of determining the dipole orientation was to observe the effect of an applied uniaxial stress on the dielectric constant. Previously, measurements of the effect of applied stress on the NMR signal in KCl:Li⁺²⁷ and on the optical absorption of CN⁻²⁸ and OH⁻²⁹ in a variety of alkali halides has been used to determine the orientations of these impurities.

In the present experiment, measurements on two crystals were carried out, one with stress and electric field parallel to the [100] direction ($N_F = 1.8 \times 10^{18} \text{ cm}^{-3}$) and one with stress and field parallel to the [111] direction ($N_F = 5.1 \times 10^{18} \text{ cm}^{-3}$). Frequencies of 0.1 and 1.0 kHz were used which are well below the relaxation rate. In both instances a decrease in the dielectric constant accompanied the increase in applied stress as shown in Fig. 15 where the pure-crystal contribution has been subtracted. Similar decreases in the dielectric loss were also observed. From these observations both $\langle 100 \rangle$ and $\langle 111 \rangle$ dipole orientations can be ruled out by a simple argument: All $\langle 100 \rangle$ orientations are equivalent in a [111] stress (see Fig. 16) and no splitting will occur upon application of the stress. Thus a [111] stress should have no effect on the dielectric constant for $\langle 100 \rangle$ dipoles. This same argument applies for $\langle 111 \rangle$ dipoles in a [100] stress. This argument does not apply, however, to $\langle 110 \rangle$ dipoles since all $\langle 110 \rangle$ orientations are not equivalent with respect to either a [100] stress or a [111] stress. The fact that a decrease in the dielectric

constant was observed for both stress directions implies $\langle 110 \rangle$ orientations for the dipoles in agreement with the high-field-polarization results.

It might be noted at this juncture that Wilson *et al.*³⁰ calculated off-center potential minima if the fluorine ions were displaced from the lattice sites along $\langle 111 \rangle$ directions. They did not calculate the effect of moving the ions out along $\langle 110 \rangle$ directions to see if an even deeper minimum would be found. Thus the present results are not in contradiction with their calculations.

The observed change in dielectric constant with applied stress allows a determination of the stress coupling coefficients β_i defined by Kanzig³¹ as $\Delta_i = \beta_i X$, where X is the applied stress and Δ_i is the stress-produced energy difference. For $\langle 110 \rangle$

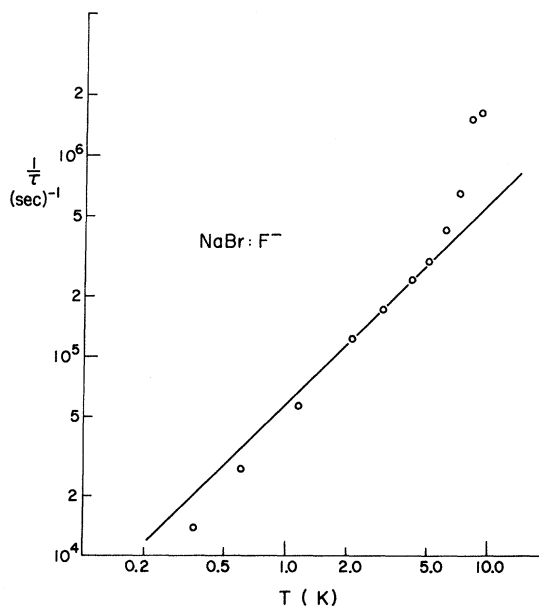


FIG. 13. Dielectric relaxation rate for NaBr:F⁻. $N_F = 1.8 \times 10^{18} \text{ cm}^{-3}$.

dipole orientations four β_i can be defined. From present measurements two of these can be determined, β_1 for [111] stress and β_4 for [100] stress.

In Fig. 17 it is seen that for both [100] and [111] stress directions the twelve $\langle 110 \rangle$ orientations fall into two groups, one of which has dipole orientations perpendicular to the stress direction. The fact that the dielectric constant decreases with increasing stress indicates that the electrically inactive orientations with dipole moment perpendicular to the applied stress and electric field (filled circles) go to lower energy. By a consideration of the Boltzmann factors for the various orientations the stress dependence of the dielectric constant can be calculated. Writing the change in energy due to the applied electric field as $\delta = \mu_0 E \cos \theta$, where θ is the angle between the field and the dipole, and the splitting due to the stress as Δ , the induced polarization for [100] fields is

$$P = N\mu_0 \cos \theta \frac{4e^{-(\Delta-\delta)/kT} - 4e^{-(\Delta+\delta)/kT}}{4 + 4e^{-(\Delta-\delta)/kT} + 4e^{-(\Delta+\delta)/kT}} .$$

Since $\delta \ll kT$, the exponentials can be expanded. The derivative with respect to field then yields the dipole contribution to the dielectric constant as a function of stress

$$\Delta\epsilon = \frac{N_F \mu_0^2}{3kT} \frac{3}{e^{\Delta/kT} + 2} , \quad (1a)$$

where the value of $\cos \theta = 1/\sqrt{2}$ has been used. For [111] stress and field, the expression is

$$\Delta\epsilon = \frac{N_F \mu_0^2}{3kT} \frac{2}{e^{\Delta/kT} + 1} . \quad (1b)$$

A fit of these expressions to the data determines the values of β_1 and β_4 . For the [100] data the fit was very good, as shown by the solid line in Fig. 15, giving a value for β_4 of

$$\beta_4 = 2.1 \times 10^{-24} \text{ cm}^3 .$$

The [111] data gave a considerably poorer fit as shown by the two lines for the 0.1-kHz data, one chosen to fit the low-stress data and one to fit the high-stress data. Using these fits as limits, the value for β_1 was found to be

$$\beta_1 = (0.7 \pm 0.2) \times 10^{-24} \text{ cm}^3 .$$

The poorness of the fit may be due to the fact that this sample represented the highest concentration of fluorine ions which could be grown into a crystal, and showed some evidence for electric dipole-dipole interactions.

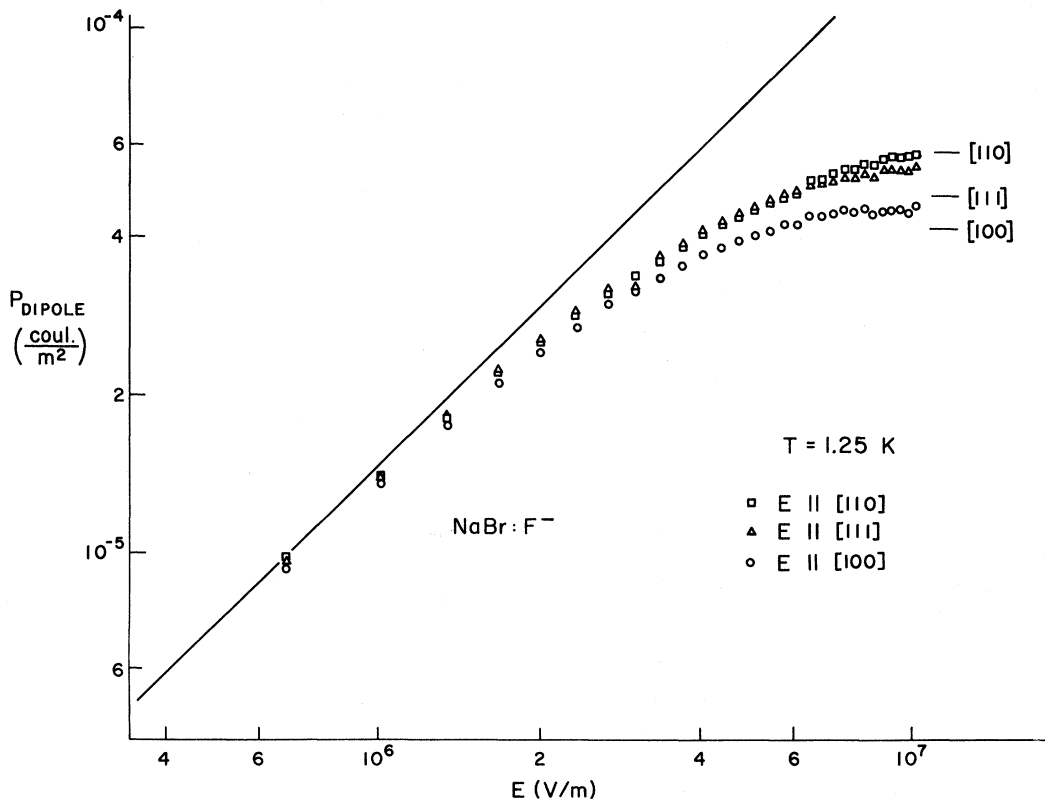


FIG. 14. Fluorine-ion contribution to the dc polarization for NaBr : F⁻. $N_F = 5.1 \times 10^{18} \text{ cm}^{-3}$.

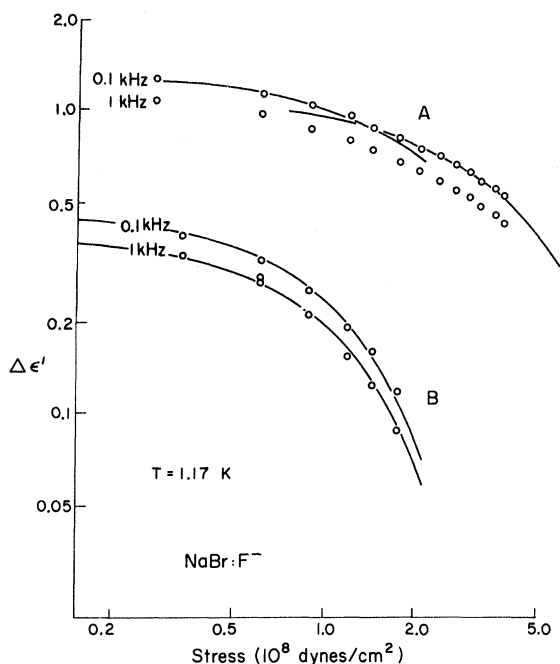


FIG. 15. Stress dependence of fluorine-ion contribution to the dielectric constant in NaBr:F⁻. (A) $N_F = 5.1 \times 10^{18} \text{ cm}^{-3}$. Stress and electric field in [111] direction. The solid lines are given by Eq. (1b). (B) $N_F = 1.8 \times 10^{18} \text{ cm}^{-3}$. Stress and electric field in [100] direction. The solid lines are given by Eq. (1a).

III. COMPARISON WITH TUNNELING MODEL

A. Modification of Simple Model

In Sec. II it was shown that the substitutional fluorine ion in NaBr makes a Langevin-Debye contribution to the dielectric constant down to low temperatures. This implies that a dipole moment having low-lying energy levels is associated with this ion.³² Low-temperature specific-heat measurements confirmed the existence of these levels. By dielectric-relaxation measurements the reorientation rate was found to increase linearly with temperature up to a temperature of 5 K. Equilibrium orientations of the dipole moment were shown to be along the $\langle 110 \rangle$ directions.

All of this evidence strongly suggests that the fluorine ion tunnels between potential minima displaced from the lattice site in the $\langle 110 \rangle$ directions. When the results are compared with the simple tunneling model used to describe KCl:Li⁺, however, two important differences are noted: (i) The specific-heat peak of the impurity ion is considerably broader in NaBr:F⁻, particularly on the low-temperature side, and (ii) the relaxation rate of the impurity ion is at least three orders of magnitude slower in NaBr:F⁻.

It seems impossible to accommodate these differ-

ences in the simple tunneling model used to describe the KCl:Li⁺ system. This can be seen most clearly in the specific-heat results. For an ion tunneling between equivalent off-center sites the ground state is split into a few levels whose separation is determined by the tunneling matrix element, the same for all ions.³³ Thus the contribution of the impurity ions to the specific heat will be of the Schottky form. In contrast to this the fluorine-ion contribution to the specific heat shows a very broad peak decreasing linearly rather than exponentially below the peak. The large contribution to the specific heat at the lowest temperature indicates that there are a number of ions with very small energy level splittings.

If the wells are made inequivalent, for example by lattice strains, additional splitting of the levels occurs which may result in a broadening of the specific-heat contribution. This was demonstrated in a calculation by Pompi and Narayanamurti³⁴ in which two of the six $\langle 100 \rangle$ wells of the CN⁻ ion in RbCl were separated in energy from the other four by the addition of a noncubic term to the potential. It was assumed that this term arose from lattice strains. The resulting broad double-humped specific-heat curve gave a rather good fit to the data of Harrison *et al.*³⁵ Although this perturbation produces a considerable broadening of the specific heat, it does not give the very smooth linear temperature dependence observed in NaBr:F⁻. However, if the strain splitting were to vary from ion to ion, the energy level distribution would be spread out, resulting in an increased breadth and smoothness of the specific heat. That this may in fact be occurring is evident in the RbCl:CN⁻ data which are somewhat broader and less peaked than the calculation.

A rough idea of the energy level distribution needed to fit the NaBr:F⁻ data at low temperatures can be gotten by a consideration of the Debye specific-heat model. In the Debye model a T^3 temperature dependence of the specific heat at low temperatures results from a density of states varying as the square of the energy.¹³ It can easily be seen that a density of states which is independent of energy will result in a linear specific-heat contribution, as observed in NaBr:F⁻. This density of states is clearly different from the δ -function distribution for the simple tunneling model.

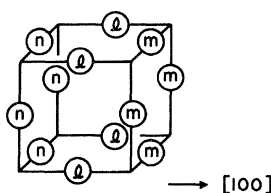


FIG. 16. Labeling of $\langle 110 \rangle$ orientations for the fluorine dipole in NaBr:F⁻.

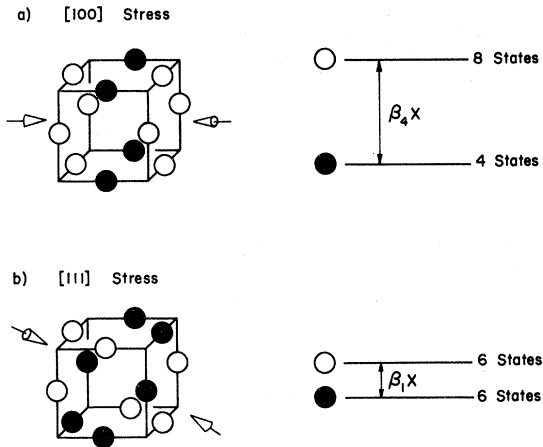


FIG. 17. Energy splitting of the fluorine-dipole orientations (indicated by balls) under the application of [100] and [111] stress.

The other instance in which the present results differ markedly from the tunneling observed in KCl: Li⁺ is the impurity-lattice relaxation rate. Although energy level separations of comparable magnitude occur in both systems as demonstrated by the heat capacity which peaks at ~ 0.5 K, the relaxation rate in NaBr: F⁻ is at least three orders of magnitude slower. Another system in which a slow reorientation occurs through tunneling is KI: O₂⁻. By means of electron spin resonance Kanzig³¹ and Silsbee³⁶ measured the reorientation of the O₂⁻ molecule following the application or removal of stress. Although the slowness of the relaxation precluded a direct measure of the ground-state splittings, Silsbee estimated a value $\leq 2\frac{1}{2}$ K caused by strains. A theory employing weak tunneling in the presence of lattice strains first proposed by Sussmann³⁷ and later developed by Pirc, Zeks, and Gosar³⁸ has been used to give a good fit to the data in the region of single-phonon relaxation. It is shown that the relatively widely separated strain-split levels relax slowly due to a small tunneling matrix element.

The above examples of the effects of strain suggest that the model to be used in describing NaBr: F⁻ is one in which a small tunneling matrix element connects wells made inequivalent by internal lattice strains. The general features of such a system can be shown with a simple two-well model which will be described next. Following this the generalization to twelve $\langle 110 \rangle$ wells will be discussed.

The problem of inequivalent wells is most easily solved by first solving the equivalent-well problem and using these solutions as a basis when the wells are made inequivalent. The double-well harmonic-oscillator potential shown in Fig. 18(a) can be writ-

ten

$$V = \begin{cases} \frac{1}{2} m \omega^2 (x + x_0)^2, & x < 0 \\ \frac{1}{2} m \omega^2 (x - x_0)^2, & x > 0 \end{cases}$$

where ω is the frequency of the particle in a single well. Since we are interested in low-temperature behavior, it will be assumed that $kT \ll \hbar\omega$ and therefore only the ground states of the two wells need be considered. These will be denoted by $|a\rangle$ and $|b\rangle$ for the left- and right-hand wells, respectively. The secular equation is

$$\begin{vmatrix} E_0 - E & \eta - SE \\ \eta - SE & E_0 - E \end{vmatrix} = 0,$$

where

$$E_0 = \langle a | H | a \rangle = \langle b | H | b \rangle,$$

$$\eta = \langle a | H | b \rangle,$$

$$S = \langle a | b \rangle.$$

This equation has the solutions

$$E = (E_0 \pm \eta) / (1 \pm S).$$

If the barrier between the wells is large compared to the zero-point energy, the overlap S will be $\ll 1$. In this case the solution can be simplified to³⁹

$$E_1 = \frac{1}{2} \hbar \omega + \Gamma,$$

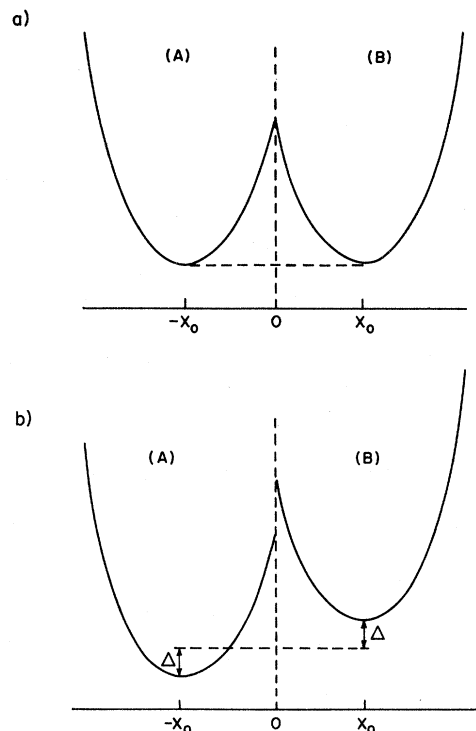


FIG. 18. Double-well harmonic oscillator. (a) Wells equivalent; (b) wells inequivalent.

with eigenfunction

$$|1\rangle = (1/\sqrt{2})(|a\rangle - |b\rangle),$$

and

$$E_2 = \frac{1}{2}\hbar\omega - \Gamma,$$

with eigenfunction

$$|2\rangle = (1/\sqrt{2})(|a\rangle + |b\rangle),$$

where

$$\Gamma = \hbar\omega\alpha_0(m\omega/\pi\hbar)^{1/2}e^{-(m\omega/\hbar)x_0^2}.$$

The energy splitting due to the tunneling is $E_1 - E_2 = 2\Gamma$, and thus Γ is called the tunnel splitting.

We now make the wells inequivalent as shown in Fig. 18(b), with the curvature of the wells remaining constant. This difference in energy of 2Δ is envisioned as arising from the presence of lattice strains. Assuming as before that $S \ll 1$, the secular equation can be written

$$\begin{vmatrix} E_1 - E & -\Delta \\ -\Delta & E_2 - E \end{vmatrix} = 0,$$

with solution

$$\begin{aligned} E_I &= \frac{1}{2}\hbar\omega - (\Gamma^2 + \Delta^2)^{1/2}, & |I\rangle &= \alpha|1\rangle + \beta|2\rangle, \\ E_{II} &= \frac{1}{2}\hbar\omega + (\Gamma^2 + \Delta^2)^{1/2}, & |II\rangle &= -\beta|1\rangle + \alpha|2\rangle, \\ \alpha, \beta &\geq 0, & \alpha^2 + \beta^2 &= 1, \\ \frac{\alpha^2}{\beta^2} &= \frac{(\Gamma^2 + \Delta^2)^{1/2} + \Gamma}{(\Gamma^2 + \Delta^2)^{1/2} - \Gamma}. \end{aligned}$$

If $\Delta = 0$, the symmetric and antisymmetric solutions $|2\rangle$ and $|1\rangle$ are restored, as they must be. For $\Delta \gg \Gamma$, the solutions are given to first order in Γ/Δ by

$$\begin{aligned} |I\rangle &\approx |a\rangle + (\Gamma/2\Delta)|b\rangle, & E_I &\approx \frac{1}{2}\hbar\omega - \Delta, \\ |II\rangle &\approx -|b\rangle + (\Gamma/2\Delta)|a\rangle, & E_{II} &\approx \frac{1}{2}\hbar\omega + \Delta. \end{aligned} \quad (2)$$

The effect of a large strain is to nearly localize the particle in one well with only a small fraction $\Gamma/2\Delta$ of the wave function in the other well. The energy difference between the states is $\approx 2\Delta$, with the tunneling only contributing a small amount of order Γ^2/Δ , which is neglected.

As shown by Sussmann³⁷ phonons may induce transitions between these states by means of their fluctuating strain which produces a fluctuating component $\delta\Delta$ in the splitting of the wells. Following Sussmann, the single-phonon relaxation is calculated by expressing the strain between the wells in terms of the phonons,

$$\epsilon_{xx} = \sum_s i \left(\frac{\hbar\omega_s}{2\rho V c_s^2} \right)^{1/2} G_s (a_s - a_s^\dagger),$$

where a_s^\dagger and a_s are the creation and annihilation operators of a phonon with frequency ω_s and velocity c_s . V and ρ are the crystal volume and den-

sity and G_s is a geometrical factor of order unity involving the phonon polarization and propagation directions. In writing this expression it is assumed that the phonon wavelength is large compared to the distance between the two wells. The strain in turn produces a fluctuating energy difference between the wells given by $\delta\Delta = b\epsilon_{xx}$, where b is the strain coupling coefficient. The transition matrix elements are calculated using $\delta\Delta$ and the initial and final states which are products of the defect state, $|I\rangle$ or $|II\rangle$, and the lattice-phonon state. Using the Debye density of phonon states the transition probability for phonon absorption is

$$W_{\text{abs}} = \frac{\Gamma^2 b^2 \langle G_s^2 \rangle}{2\pi\rho\hbar^4 c^5} \left[e^{\Delta E/kT} - 1 \right],$$

where $\Delta E = E_{II} - E_I$ and $\langle G_s^2 \rangle$ is the average of the geometry factor G_s^2 over all polarizations and propagation directions for phonons of energy ΔE . Note that aside from the term in square brackets there is no dependence of the transition probability on the energy difference ΔE . This results from the decrease in the transition matrix element caused by the increasing localization of the ion with strain being compensated by an increasing phonon density of states, as pointed out by Silsbee.³⁶

Using standard rate theory, the relaxation rate is calculated to be

$$1/\tau = W_{\text{abs}}(1 + e^{\Delta E/kT}).$$

For $kT \gg \Delta E$, the exponentials can be expanded, resulting in

$$\frac{1}{\tau} \approx \frac{\Gamma^2 b^2 \langle G_s^2 \rangle}{\pi\rho\hbar^4 c^5},$$

showing the linear temperature-dependence characteristic of one-phonon relaxation. At higher temperatures multiphonon relaxation will cause the relaxation rate to increase more rapidly than T . The expressions for multiphonon relaxation are rather complex, and the present data are not sufficiently detailed to warrant consideration of these processes here.

To generalize this expression to the case of twelve $\langle 110 \rangle$ wells, the expression for the transition probability must be modified to include the greater variety of possible well orientations. The result as quoted by Pirc *et al.*³⁸ is

$$W_{\text{abs}} = \frac{\Gamma^2 b^2}{3\pi\rho\hbar^4 c^5} \frac{\Delta E}{e^{\Delta E/kT} - 1}, \quad (3)$$

where

$$b^2 = \frac{1}{4} \left(\frac{2\beta_4}{S_{11} - S_{12}} \right)^2 + \frac{1}{2} \left(\frac{3\beta_1}{S_{44}} \right)^2$$

and $S_{11} - S_{12}$ and S_{44} are the elastic compliance constants of the pure lattice. This expression for b^2 applies when the impurity tunnels by 60° . For

(110) wells tunneling can also occur through 90° across the face of the cube (see Fig. 16). Tunneling by 60° involves a shorter path length and would therefore usually be larger. Since the measurements discussed here are insensitive to which type of tunneling is taking place, for simplicity only 60° tunneling is assumed.

The relaxation rate is most easily related to the transition probability in the case where the ion is nearly localized by the strains. It will be shown in Sec. III B that this is the case for NaBr : F⁻. Under these conditions transitions from one state to another can be looked at as transitions from one well to another. Since the dielectric constant is the quantity measured, we will be interested in the transition rates between wells which contribute to the polarization for a given field direction. For a [100] field Fig. 16 shows that the l wells have dipole moments perpendicular to the field and thus do not contribute to the polarization although transitions between the m and n wells take place by tunneling through the l wells. The expression for the transition rates is rather complicated since an ion in a particular m well may tunnel to either of the two l wells which may be of different energy due to strains. At low temperatures the transition probabilities will not in general be equal and there will be no single relaxation rate. At higher temperatures, however, the transition rates become independent of the well energy difference. The rate equation between wells m and n can then be easily written

$$\frac{d(m-n)}{dt} = -2W(m-n),$$

where m and n are the well populations. Thus the relaxation rate is, using Eq. (3) and assuming $kT \gg \Delta E$,

$$\frac{1}{\tau} = 2W = \frac{2\Gamma^2 b^2 k T}{3\pi \rho \hbar^4 c^5}. \quad (4)$$

B. Comparison with Data

We will now go back and see to what extent the differences between the NaBr : F⁻ data and the simple tunneling model can be reconciled by the modification to the model just discussed. One of these differences was the broad specific-heat contribution of the fluorine ions with a linear temperature dependence at low temperatures. It was pointed out at the beginning of Sec. III A that to account for the linear temperature dependence a region in the density of states roughly independent of energy is required. As shown in Eq. (2) in the limit where $\Gamma \ll \Delta$ the splitting of the ground state is approximately independent of the tunneling matrix element and proportional to the strain energy. In the case of twelve (110) wells the level structure will of

course be more complex. The important point is that for $\Gamma \ll \Delta$ the splitting will be proportional to Δ . Thus while tunneling alone will not provide the distribution of energy levels required the random variation of the internal strain will produce a broad energy level distribution in the limit of a small tunneling matrix element.

It is difficult to predict the shape of the level distribution since the splittings depend both on the strain magnitude and direction. For example, a strain in the [100] direction will split the tunneling states into two levels of fourfold and eightfold degeneracy (see Fig. 17). Deviations of the strain from the [100] direction will further split these levels, with the amount of splitting depending on the component of the strain perpendicular to the [100] axis. To get an empirical picture of the level distribution, the specific-heat integral

$$C(T) = \int_0^\infty C(\Delta/kT) \eta(\Delta) d\Delta$$

was numerically evaluated using the Schottky expression for $C(\Delta/kT)$. For the density of states $\eta(\Delta)$, a number of expressions were used including (a) a flat distribution, $\eta(\Delta) = \eta_0$ for $\Delta \leq \Delta_M$, $\eta(\Delta) = 0$ for $\Delta > \Delta_M$, (b) a distribution which was flat up to $\Delta = \frac{1}{2}\Delta_M$ and then decreased linearly to zero at $\Delta = \Delta_M$, (c) a distribution decreasing linearly from η_0 at $\Delta = 0$ to zero at $\Delta = \Delta_M$, and (d) a Gaussian distribution,

$$\eta(\Delta) = \eta_0 e^{-\Delta^2/\Delta_M^2}.$$

All of these distributions gave a qualitatively similar temperature dependence for the specific heat, varying approximately linearly at low temperatures and passing through a relatively broad peak. Distributions (a) and (b) gave curves which were almost indistinguishable from each other. Likewise, distributions (c) and (d) gave very similar curves which had a somewhat broader peak and deviated from a linear temperature dependence at a lower temperature than the curve for (a) and (b). The curves were fit to the data by adjusting Δ_M to get the peaks at the right temperature. Expressions (a) and (b) seemed to give the best fit, shown by the solid lines in Fig. 7. Determining the best fit was somewhat difficult since the discrimination was made on the basis of the data at and above the peak temperature where the uncertainty is greatest due to the large value of the pure-crystal specific heat which must be subtracted.

The values of Δ_M/k needed to fit the data ranged from about 1.5 K for the lowest-concentration sample to 3 K for the highest-concentration sample. Using the stress-coupling coefficients the stresses corresponding to these splittings are $2-4 \times 10^8$ dyn/cm². These are rather large values for internal stresses although values of the same order of magnitude were calculated by Sussmann³⁷ and Sils-

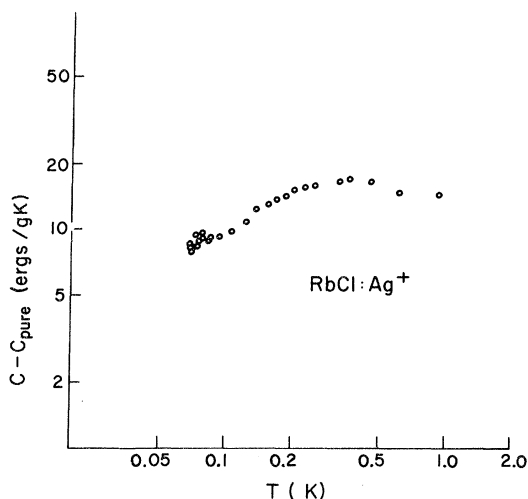


FIG. 19. Specific heat of $\text{RbCl}:\text{Ag}^+$ with the pure-crystal contribution subtracted. $N_{\text{Ag}} = 1.9 \times 10^{18} \text{ cm}^{-3}$.

bee³⁶ for the O_2^- molecule.

It was pointed out in Sec. II that the entropy calculated from the specific heat increased with concentration from $S/N_F k = 1.05 = \ln 2.9$ to $S/N_F k = 1.66 = \ln 5.3$. For an impurity tunneling between twelve positions, a value of $S/N_F k = \ln 12$ would be expected for all concentrations. Although no clear-cut resolution to this discrepancy can be given, the following argument is put forward. In calculating the entropy from the specific heat, it was assumed that the specific heat never rose above the linear temperature dependence at temperatures lower than 50 mK. It may be that this assumption is incorrect. In order for the specific heat to decrease linearly, the density of states must remain approximately constant. A constant density of states is envisioned as arising from a random strain splitting of the ground state. However, the strain is even and therefore cannot split the levels for wells with inversion symmetry. Thus one would expect a spike in the density of states due to the levels which are not split by the strain. This spike will occur at an energy equal to the tunnel splitting between the degenerate wells which is too small to be seen in the heat capacity above 50 mK (see below). This inversion degeneracy will vary between 2 and 8 depending on the orientation of the strain at a particular site (see Fig. 17). Thus the entropy should be $\leq N_F k \ln 6$, as observed.

The discussion of relaxation in Sec. III A showed that there should be a temperature range in which the relaxation rate is linearly proportional to the temperature due to single-phonon relaxation. In Fig. 13 it is seen that indeed such a temperature dependence was observed below 5 K. Above 5 K the more rapid rate characteristic of multiphonon relaxation is observed. Below 2 K the slight deviation

from linearity may indicate that the temperature is comparable to the strain splitting and that the simple expression for the relaxation rate is no longer valid.

As shown in Eq. (4) in the linear region the relaxation rate is proportional to the tunneling matrix element. All other parameters in this expression are known, and thus the measured relaxation rate can be used to calculate a value for the tunneling matrix element. Using elastic compliance constants derived from the elastic constants of Lewis *et al.*,¹⁴ the stress-coupling coefficients calculated in Sec. II, and the Debye sound velocity, the tunneling matrix element is calculated to be

$$\Gamma = 1.2 \times 10^{-18} \text{ erg},$$

$$\Gamma/k = 8.7 \text{ mK}.$$

This is indeed small compared to the strain energies, justifying the assumption of nearly localized ions. It is this small tunneling matrix element which makes the relaxation in $\text{NaBr}:\text{F}^-$ slow compared to that of $\text{KCl}:\text{Li}^+$ where $\Gamma/k = 1.2 \text{ K}$.²⁰

The small tunneling matrix element also explains why levels split by this amount would not give a significant contribution to the specific heat at 50 mK. Since Γ represents an upper limit to the tunnel splitting of the inversion degenerate wells (in most cases the degenerate wells will be connected only by tunneling of greater than 60° and will therefore have smaller splittings), it is reasonable that no deviation from linearity was observed in the low-temperature specific heat. It might also be noted that the smaller tunneling matrix elements for the degenerate levels will result in a slower relaxation rate making detection of these levels by other means difficult.

IV. SIMILAR SYSTEMS

It is interesting to look for other systems to which the model discussed in the present paper might be applicable. One system which has many of the same properties as $\text{NaBr}:\text{F}^-$ is the system $\text{RbCl}:\text{Ag}^+$. Early thermal-conductivity measurements showed no decrease in the low-temperature conductivity for RbCl crystals doped with AgCl .⁴⁰ Measurements of paraelectric cooling by Kapphan and Lüty⁴¹ indicated that the Ag^+ impurities were tunneling between $\langle 111 \rangle$ off-center wells. The specific heat of $\text{RbCl}:\text{Ag}^+$, shown in Fig. 19, revealed a broad low-temperature peak contributed by the silver ions. The shape of the peak is qualitatively similar to that observed for $\text{NaBr}:\text{F}^-$. By means of dielectric relaxation the relaxation rates shown in Fig. 20 were obtained. Good agreement is found with the value calculated by Kapphan and Lüty from paraelectric cooling data at 1.4 K. A rather broad distribution of relaxation rates was observed, par-

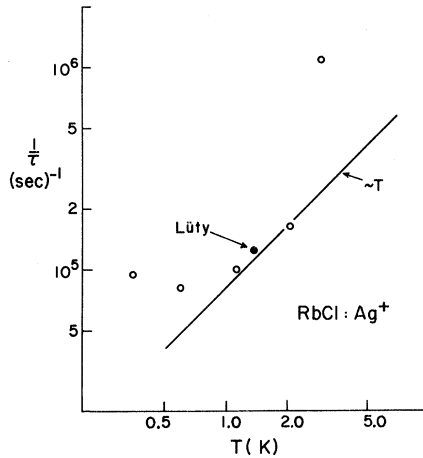


FIG. 20. Dielectric relaxation rate for RbCl:Ag⁺. $N_{Ag} = 1.9 \times 10^{18} \text{ cm}^{-3}$. Filled circle indicates value quoted by Kapphan and Lity (Ref. 41).

ticularly at the lowest temperatures, making the points in Fig. 20 below about 1 K rather uncertain. Recent measurements of paraelectric relaxation by Bridges⁴² have shown a rather broad resonance with a dependence on frequency indicating a small zero-field splitting. Bridges quotes an upper limit for the tunnel splitting of 0.14 K. These observations are consistent with the model of a small tunneling energy in a strained lattice. From the relaxation rate a tunneling matrix element of the same order of magnitude as that observed in NaBr:F⁻ seems likely.

Other systems for which this model might be appropriate are RbCl:OH⁻ and KCl:OH⁻. Thermal conductivity in RbCl:OH⁻²² indicates rather weak phonon scattering, and the heat-capacity⁹ exhibits a broad peak with linear temperature dependence below the peak.⁴³ The heat-capacity contribution of the OH⁻ ion in KCl is also considerably broader than that of a Schottky term,⁴⁴ indicating that strains may be playing a role. On the other hand, the dipole-lattice relaxation is large, as evidenced from dielectric and thermal conductivity measurements, which implies a large tunneling matrix element. In the case of this ion, the possibility of a combined center-of-mass and a rotational motion further complicates the interpretation of the data.

V. CONCLUSION

Fluorine ions in NaBr have associated with them large dipole moments with low-lying energy levels. The dipoles were found to have equilibrium orientations in the $\langle 110 \rangle$ directions. Debye dielectric relaxation was observed with the relaxation rate increasing linearly with temperature for temperatures less than 5 K. From these observations it was concluded that the fluorine ions tunnel between

potential minima displaced in the $\langle 110 \rangle$ directions from the center of the lattice cavity.

The data, however, exhibited two important departures from the behavior observed for a simple tunneling system such as KCl:Li⁺. These were (i) a much broader low-temperature specific-heat contribution of the impurity ions and (ii) an impurity-lattice relaxation rate slower by at least three orders of magnitude. To explain these differences it was necessary to consider a modified tunneling model in which the wells between which the ion tunnels are of different energy. This difference in energy was assumed to arise from random lattice strains. It was shown that in the limit of a small tunneling matrix element it is the strain splitting which determines the low-lying-energy-level structure. Thus the observed breadth of the specific-heat peak was a result of the variation of the internal strain from one site to another, while the slow relaxation rate was due to the small size of the tunneling matrix element connecting the wells. The fact that the effect of strains was not apparent in the data for KCl:Li⁺ is due to the large tunneling matrix element for this system which dominates the strain splitting in determining the low-lying-energy-level structure.

Several other systems with properties similar to NaBr:F⁻ were discussed, namely, RbCl:Ag⁺, RbCl:OH⁻, and KCl:OH⁻. In all of these systems the specific-heat contribution of the impurity is considerably broader than that of a Schottky term. In view of the model used for NaBr:F⁻ it is clear that the deduction of a tunnel splitting from the temperature dependence of the specific heat must be done with extreme care since for small tunneling the energy-level structure giving rise to the specific heat will be nearly independent of the magnitude of the tunneling matrix element. It is seen that the KCl:Li⁺ system represents a limiting case in which the tunneling plays the dominant role in determining the low-lying-energy-level structure allowing the specific heat to be interpreted in terms of the tunneling matrix element.

It was assumed in the discussion of the model that the energy difference between the wells arose from lattice strains. This may not be the only mechanism present. Indeed, the large value of internal strain needed to explain the specific-heat data suggests that perhaps some other mechanism is contributing to this difference. The data presented are sensitive to the fact that differences exist between the well energies but do not give an indication as to the origin of these differences. A very careful annealing study might help to resolve this question.

Finally, it must be concluded that a small tunnel splitting alone is not sufficient to produce an effective paraelectric-cooling device. The strong

effect of lattice strains on the low-lying energy levels produces a large zero-field splitting, severely limiting the lowest temperatures which may be attained by paraelectric cooling.

ACKNOWLEDGMENTS

The author would like to thank Professor R. O. Pohl for his guidance and encouragement throughout the course of this investigation. He also thanks

Professor R. H. Silsbee for originally suggesting the strained tunneling model and for many stimulating conversations. Thanks are also due to D. J. Channin, A. T. Fiory, and V. Narayanamurti for many valuable discussions. G. Schmidt gave invaluable assistance in providing the excellent NaBr crystals. The results prior to publication of S. Kapphan and F. Lüty are also gratefully acknowledged.

*Work mainly supported by the Materials Science Center at Cornell University.

†Present address: Department of Physics, University of Washington, Seattle, Wash. 98105.

¹V. Narayanamurti and R. O. Pohl, *Rev. Mod. Phys.* **42**, 201 (1970), and references contained therein.

²S. Kapphan, Ph.D. thesis (University of Utah, 1970) (unpublished); S. Kapphan, F. Lüty, and K. Weinmann (unpublished).

³G. Lombardo and R. O. Pohl, *Bull. Am. Phys. Soc.* **11**, 212 (1966).

⁴J. P. Harrison, *Rev. Sci. Instr.* **39**, 145 (1968).

⁵W. D. Seward, Ph. D. thesis (Cornell University, 1965) (unpublished); Materials Science Center Report No. 368, 1965 (unpublished).

⁶P. D. Thacher, Ph.D. thesis (Cornell University, 1965) (unpublished); Materials Science Center Report No. 369, 1965 (unpublished).

⁷E. Gmelin, *Cryogenics* **7**, 225 (1967).

⁸R. O. Pohl, V. L. Taylor, and W. M. Goubau, *Phys. Rev.* **178**, 1431 (1969).

⁹A. T. Fiory, *Phys. Rev. B* **4**, 614 (1971).

¹⁰J. M. Peech, D. A. Bower, and R. O. Pohl, *J. Appl. Phys.* **38**, 2166 (1967).

¹¹M. V. Klein, S. O. Kennedy, Tan Ik Gie, and Brent Wedding, *Mat. Res. Bull.* **3**, 677 (1968).

¹²M. F. O'Brien, Masters thesis (Cornell University, 1969) (unpublished); Materials Science Center Report No. 1167, 1969 (unpublished); M. F. O'Brien and R. H. Plovnick, *Mat. Res. Bull.* **4**, 671 (1969).

¹³C. Kittel, *Introduction to Solid State Physics*, 3rd ed. (Wiley, New York, 1966), p. 178.

¹⁴J. T. Lewis, A. Lehoczky, and C. V. Briscoe, *Phys. Rev.* **161**, 877 (1967).

¹⁵J. P. Harrison, G. Lombardo, and P. P. Peressini, *J. Phys. Chem. Solids* **29**, 557 (1968).

¹⁶M. Gomez, S. P. Bowen, and J. A. Krumhansl, *Phys. Rev.* **153**, 1009 (1967).

¹⁷G. Lombardo and R. O. Pohl, *Phys. Rev. Letters* **15**, 291 (1965).

¹⁸H. S. Sack and M. C. Moriarty, *Solid State Commun.* **3**, 93 (1965).

¹⁹R. J. Rollefson and R. O. Pohl, *Bull. Am. Phys. Soc.* **14**, 348 (1969).

²⁰J. P. Harrison, P. P. Peressini, and R. O. Pohl, *Phys. Rev.* **171**, 1037 (1968).

²¹F. C. Baumann, J. P. Harrison, R. O. Pohl, and W. D. Seward, *Phys. Rev.* **159**, 691 (1967).

²²R. L. Rosenbaum, Ph.D. thesis (University of Illinois, 1968) (unpublished).

²³R. J. Rollefson and R. O. Pohl, *Bull. Am. Phys. Soc.* **15**, 605 (1970).

²⁴Two measurements have been made of the relaxation

rate for KCl:Li⁺. By measuring the dependence of paraelectric cooling on the rate at which the field was removed Kapphan and Lüty (Ref. 41) calculated a relaxation rate at 1.4 K of $1.0 \times 10^8 \text{ sec}^{-1}$. W. Goubau and R. O. Pohl [*Bull. Am. Phys. Soc.* **16**, 356 (1971)] deduce a lower limit to the relaxation rate of $1.2 \times 10^8 \text{ sec}^{-1}$ by observing the magnitude of the phonon pulse produced when a pulsed electric field of variable length is applied to the crystal [W. M. Goubau (unpublished)].

²⁵U. Bosshard, R. W. Dreyfus, and W. Kanzig, *Physik Kondensierten Materie* **4**, 254 (1965).

²⁶V. V. Daniel, *Dielectric Relaxation* (Academic, New York, 1967), Chap. 7.

²⁷D. W. Alderman and R. M. Cotts, *Phys. Rev. B* **1**, 2870 (1970).

²⁸W. D. Seward and V. Narayanamurti, *Phys. Rev.* **148**, 463 (1966).

²⁹H. Härtel and F. Lüty, *Phys. Status Solidi* **12**, 347 (1965).

³⁰W. D. Wilson, R. D. Hatcher, G. J. Dienes, and R. Smoluchowski, *Phys. Rev.* **161**, 888 (1967).

³¹W. Kanzig, *J. Phys. Chem. Solids* **23**, 479 (1962).

³²J. H. Van Vleck, *The Theory of Electric and Magnetic Susceptibilities* (Oxford U. P., Oxford, England, 1932), Chap. VII.

³³It might be thought that the tunneling matrix element would vary due to lattice strains. Pirc *et al.* (Ref. 38) have shown by a WKB calculation that the tunneling matrix element should be very insensitive to lattice strain. From the observed linear temperature dependence of the relaxation rate of OH⁻ in several alkali halides B. G. Dick [*Solid State Commun.* **8**, 777 (1970)] estimates that the maximum change in the tunneling matrix element for the strains possible in alkali halides is less than a few percent.

³⁴R. L. Pompei and V. Narayanamurti, *Solid State Commun.* **6**, 645 (1968).

³⁵J. P. Harrison, P. P. Peressini, and R. O. Pohl, *Phys. Rev.* **167**, 856 (1968).

³⁶R. H. Silsbee, *J. Phys. Chem. Solids* **28**, 2525 (1967).

³⁷J. A. Sussmann, *Physik Kondensierten Materie* **2**, 146, (1964).

³⁸R. Pirc, B. Zeks, and P. Gosar, *J. Phys. Chem. Solids* **27**, 1219 (1966).

³⁹See Ref. 16. For an elementary discussion of the double-well harmonic oscillator see R. P. Feynman, R. B. Leighton, and M. Sands, *Lectures on Physics* (Addison-Wesley, Reading, Mass., 1965), Vol. III, Chap. 8.

⁴⁰In fact a small increase in the conductivity below 2 K was observed for light Ag⁺ doping levels. A similar effect has been observed for Ag⁺ in KCl, as discussed by F. C. Baumann and R. O. Pohl [*Phys. Rev.* **163**, 843 (1967)].

This effect is rather small and the important point in the present context is that no large resonant scattering similar to that of KCl:Li⁺ is observed.

⁴¹S. Kapphan and F. Lüty, *Solid State Commun.* **6**, 907 (1968).

⁴²F. Bridges, *Bull. Am. Phys. Soc.* **15**, 787 (1970); and private communication.

⁴³This statement applies to the lowest-concentration sample reported in Ref. 9. For the high-concentration samples dipole-dipole interactions begin to affect the specific heat.

⁴⁴P. P. Peressini, J. P. Harrison, and R. O. Pohl, *Phys. Rev.* **182**, 939 (1969).

Photoluminescence of Radiation Defects in Ion-Implanted 6H SiC[†]

Lyle Patrick and W. J. Choyke

Westinghouse Research Laboratories, Pittsburgh, Pennsylvania 15235

(Received 15 September 1971)

Radiation defects were introduced into 6H SiC by ion implantation and by electron bombardment. The defects produce a new low-temperature luminescence that is independent of the implanted ion, and one portion, the D_1 spectrum, persists after a 1700 °C anneal. A comparison of the D_1 spectrum in ion- and electron-bombarded samples shows that its intensity is strongly dependent on defect concentration, suggesting that the luminescence center is a pure-defect complex, possibly a divacancy. The D_1 spectrum, which was previously observed in cubic SiC, has a strong vibronic structure with localized and resonant modes. In 6H SiC it is repeated three times, due to the three inequivalent sites in this polytype. D_1 has an unusual temperature dependence, the low-temperature (1.4 °K) spectrum being extinguished as the high-temperature (77 °K) form is activated. The abrupt change of spectrum is attributed to a lattice distortion at the low temperature. The changes in luminescence on annealing are correlated with changes in electrical properties observed in ion-implanted samples by Marsh and Dunlap.

I. INTRODUCTION

Ion implantation in SiC results in damage to the lattice that is difficult to repair, for some defects remain even after a 1700 °C anneal. One of these persistent defects gives rise to a strong low-temperature luminescence spectrum (the D_1 spectrum) that has a characteristic vibronic structure. The D_1 spectrum was first studied in cubic (3C) SiC, and it was shown not to depend on the implanted ion.¹ We have now subjected 6H SiC to the same damage and annealing procedures, and we have found a very similar persistent luminescence. It can be recognized as the D_1 spectrum of polytype 6H by the distinctive localized and resonant vibrational structure, but it is different from the 3C spectrum in ways that are related to differences in crystal and band structure. For example, it is repeated three times, for there are three crystallographically inequivalent lattice sites in 6H SiC.^{2,3} It is also displaced to higher photon energies by about 0.6 eV, the difference between 6H and 3C energy gaps.⁴

The most striking feature of the D_1 spectrum is its temperature dependence. In cubic SiC the appearance of the low- (L), medium- (M), and high- (H) temperature forms of the spectrum were tenta-

tively attributed to Jahn-Teller distortion. The symmetry of 6H SiC is lower (space group $P6_3mc$), and only two forms of the spectrum (called L and H) are observed. It is probable that the symmetry of the center is too low for the orbital degeneracy that leads to a true Jahn-Teller effect.⁵ Nevertheless, the replacement of the H spectrum by the L spectrum with decreasing temperature can best be attributed to a change in lattice configuration that may be called a pseudo-Jahn-Teller distortion.⁵ The H form of the spectrum was reported earlier by Makarov,⁶ but with less resolution.

The structure of the D_1 luminescence center is not known. A possible model mentioned in Ref. 1 is an impurity-vacancy pair. This choice was based on the extensive work on radiation damage and annealing in Si, where the progression from simple vacancies and interstitials to more complex defects in successive annealing stages has been well documented.⁷ The work of Watkins and co-workers on persistent defects is especially significant.⁸ We have found a number of sample-dependent spectra in 6H SiC that appear to be due to impurity-defect complexes. However, a comparison of ion- and electron-bombarded samples leads to the conclusion that the D_1 center does not depend on the presence of an impurity. A pure-defect model